Earthquake & Engineering Structural Dynamics
The Journal of the International Association for Earthquake Engineering

Non-linear dynamic soil-structure interaction for the integrated seismic assessment of structures and foundations

Journal:	*Earthquake Engineering and Structural Dynamics*
Manuscript ID	EQE-16-0105
Wiley - Manuscript type:	Research Article
Date Submitted by the Author:	21-Mar-2016
Complete List of Authors:	Figini, Raffaele; ENEL, Civil Technical Support Paolucci, Roberto; Politecnico di Milano, Structural Engineering
Keywords:	Seismic assessment, non-linear dynamic soil-structure interaction, bridge piers, shallow foundations, macro-element modeling

Non-linear dynamic soil-structure interaction for the integrated seismic assessment of structures and foundations

Figini, R.[1], Paolucci, R.[2]

[1] *ENEL, Via Adamello 5, 20099, Sesto San Giovanni, Milan, Italy*
[2] *Politecnico di Milano, P.za Leonardo da Vinci 32, 20133, Milan, Italy*

SUMMARY

This paper aims at clarifying the role of dynamic soil-structure interaction in the seismic assessment of structure and foundation, when the non-linear coupling of both subsystems is accounted for. For this purpose, the seismic assessment of an ideal set of bridge piers on shallow foundations is considered. After an initial standard assessment, based on capacity design principles, the evaluation of the seismic response of the piers is carried out by dynamic simulations, where both the non-linear responses of the superstructure and of the foundation are accounted for, in the latter case through the macro-element modeling of the soil-foundation system. The results of the dynamic simulations point out the beneficial effects of the non-linear response of the foundation, which provides a substantial contribution to the overall energy dissipation during seismic excitation, thus allowing the structural ductility demand to decrease significantly with respect to a standard fixed-base or linear-elastic base assessment. Permanent deformations at the foundation level, such as rotation and settlement, turn out to be of limited amount. Therefore, an advanced assessment approach of the integrated non-linear system, consisting of the interacting foundation and superstructure, is expected to provide more rationale and economic results than the standard uncoupled approach, which, neglecting any energy dissipation at the foundation level, generally overestimates the ductility demand on the superstructure.

KEY WORDS: Seismic assessment, non-linear dynamic soil-structure interaction, bridge piers, shallow foundations, macro-element modeling

1. INTRODUCTION

The ability of the foundation to dissipate energy during earthquakes is generally neglected in seismic design and, in most cases, it is explicitly avoided by the requirement that the foundation should undergo very limited non-linear response and permanent deformations, even under ultimate limit state verifications. This is generally accomplished by verifying that the combined application of permanent and seismic loads does not exceed the bearing capacity of the foundation.

This conservative approach, partly justified by the cost and difficulty of post-earthquake assessment and retrofit of the foundation system, may have several important drawbacks, as discussed in more detail by Pecker et al. [1]. As a matter of fact, this may typically lead to oversizing and to preventing the foundation to exploit any fraction of its energy dissipation capacity, so to reduce the seismic demand on the super-structure. This was clarified in several recent research works, both analytical and experimental (see [1], [2], [3] and [4]), which highlighted that the seismic response of the foundation system may undergo significant non-

linear effects, relying typically on: 1) limited permanent settlements and rocking; 2) substantial dissipation of input energy; 3) substantial reduction of the overall seismic demand on the superstructure.

For these reasons, several proposals were recently made to support an integrated design of foundation and super-structure, for the combined ductility capacity of both foundation and superstructure to be fully exploited (see [4], [5], [6] and [7]).

The seismic assessment of foundations of existing buildings poses even more stringent problems than design of new structures, especially in those cases, that are becoming more and more frequent in the engineering practice, where the foundation system is assessed under seismic actions larger than those considered for design, either because of an upgrade of seismic zoning or of a change of use of the building. As a consequence, retrofitting the foundation system by increasing its dimensions and strength, until the seismic bearing capacity check is satisfied, may lead to overly conservative solutions. This was recently recognized by the ASCE 41-13 Standard *Seismic Evaluation and Retrofit of Existing Buildings* [8], where load-deformation curves for shallow foundations are introduced, together with foundation ductility factors, and acceptance criteria for different performance levels are defined based on permanent settlements and rotations.

To explore the potential benefits of considering the coupled non-linear response of foundation and superstructure in the seismic assessment of structures, we considered in this paper a set of bridge piers, ideally designed within an area where no seismic regulation was initially enforced, but, owing for example to a change of seismic zoning, a seismic assessment is required. After introducing the basic concepts on the moment capacity of shallow foundations, which was found in many recent works to govern the non-linear interaction with the superstructure under seismic loading, the assessment of the four bridge piers under study is addressed. First, a standard approach is considered, based on capacity principles and neglecting the non-linear response of the foundation. Subsequently, the results of such simplified assessment approach are checked by a set of dynamic soil-structure interaction simulations, where the non-linear interaction between foundation and superstructure is accounted for and different assumptions on the foundation response are considered, i.e., fixed-base, linear-elasticbase, non-linearbase.

2. MOMENT CAPACITY OF SHALLOW FOUNDATIONS

The bearing capacity of a shallow foundation under the combined effect of vertical (N) and horizontal (V) forces, and overturning moment (M), is often introduced in terms of a failure surface that, following for example the formulation of Nova and Montrasio [9], can be expressed as:

$$\left(\frac{V}{N_{max}\mu}\right)^2 + \left(\frac{M}{N_{max}B\Psi}\right)^2 - \left(\frac{N}{N_{max}}\right)^2 \left(1 - \frac{N}{N_{max}}\right)^{2\beta} = 0 \qquad (1)$$

where N_{max} is the bearing capacity under vertical load, μ is the soil-foundation friction coefficient (typically $\mu = 3/4\tan\varphi$, where φ is soil friction angle), Ψ is related to failure under eccentric loading ($\Psi = 0.48$ according to Vesic [10]), β is a model parameter, generally close to 1.

Under seismic loading, typically when the ratio M/V is greater than the foundation width B, the response of the foundation is dominated by rocking, so that V can be neglected in eq. (1). Then,

considering $\Psi \sim 0.50$ and $\beta \sim 1$, the moment capacity M_c of the shallow foundation from eq. (1) can be written as:

$$M_c = \frac{NB}{2}\left(1 - \frac{N}{N_{max}}\right). \quad (2)$$

The failure surface corresponding to eq. (2) is displayed in Figure 1, and can be interpreted as the *M*-*N* foundation interaction domain. Note that both the ASCE 41-13 [8] and the 2015 Canadian Building Code [11] suggest a similar equation to determine M_c:

$$M_c = \frac{NB}{2}(1 - \rho_{ac}), \quad (3)$$

where $\rho_{ac} = \frac{A_c}{A} = \frac{B_c}{B} = \frac{q}{q_c}$ is defined as compression ratio, i.e. the ratio of the contact area A_c at failure (see Figure 1) to the total area A. For light foundations (N/N_{max} small), M_c tends to $NB/2$, thus corresponding to the eccentricity limit $e_{lim} = B/2$.

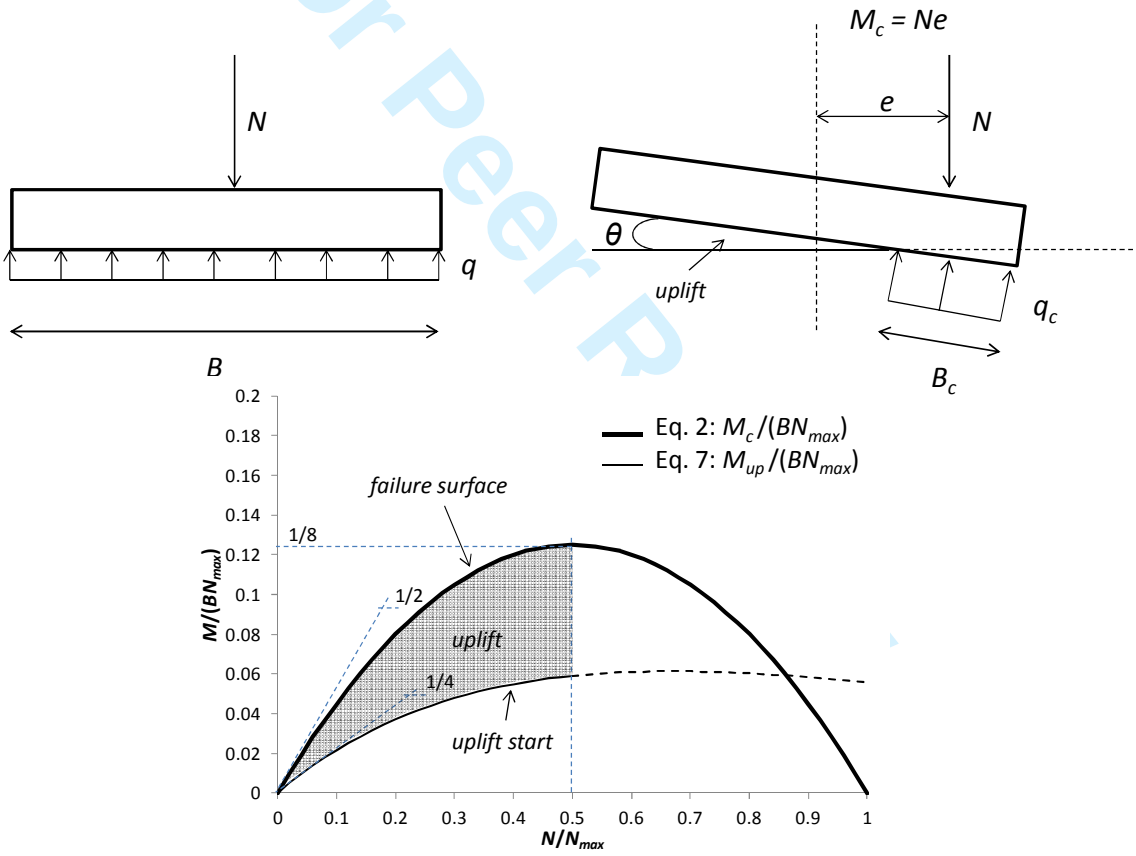

Figure 1 – Top: shallow foundation subject to centered vertical load (left) and to eccentric vertical load corresponding to the footing moment capacity M_c (right). Bottom: *M*-*N* interaction domain for shallow foundation: definition of the failure surface corresponding to M_c (eq. 2) and of the uplift initiation M_{up} (eq. 7). Uplift domain is limited to $N/N_{max} < 0.5$, which is the typical design region.

Following ASCE 41-13 [8], the M_c-θ capacity curve can be represented either by a bi-linear or by a tri-linear model, as displayed in Figure 2. In the first case, two points define the model: (θ_y-

M_y), where the ultimate surface is reached, and (θ_u-M_u), where the maximum allowable rotation θ_u is reached. In the bi-linear model: $M_y = M_u = M_c$. θ_y can be approximated by dividing M_c by the initial elastic rotational stiffness $K_{F,0}$:

$$\theta_y = \frac{M_c}{K_{F,0}}, \tag{4}$$

where $K_{F,0}$ can be evaluated either by standard formulas [12], or by empirical correlations, as suggested by Kutter et al. [8]. As an example, the rotational stiffness of a square foundation of width B, over a homogeneous halfspace with shear modulus G and Poisson ratio ν, can be expressed by [12]:

$$K_{F,0} = \frac{0.45GB^3}{1-\nu}. \tag{5}$$

The definition of θ_u is less straightforward, because it typically depends on the desired structural performance, for example in terms of limit drift. There are only few building codes which give foundation rotation limits: as an example, the Japanese Railway Code suggests to limit pier foundation rotation to 20 mrad [13]. Chapter 8 of ASCE 41-13 defines acceptance criteria for total footing rotation angles θ_u, depending on foundation shape and compression ratio, which will be used in the assessment cases illustrated within this work.

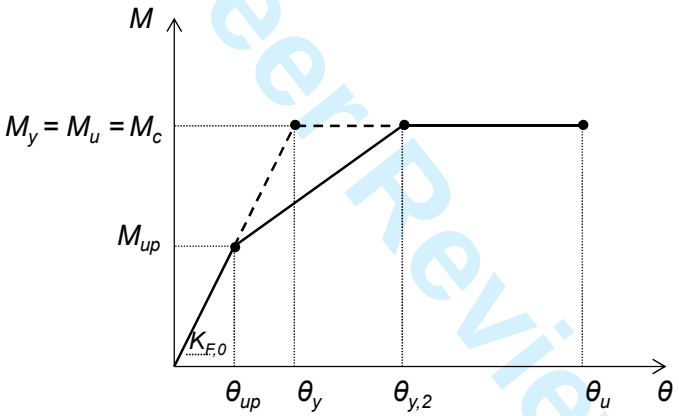

Figure 2 – Bi-linear (dashed line) and tri-linear (continuous line) simplified representations of the non-linear foundation capacity curves.

The bi-linear model may be very useful for simplified assessment purposes, because the ratio θ_u/θ_y between allowable and yield rotation, denoted in ASCE 41-13 as m-factor, can be interpreted in terms of foundation ductility:

$$m = \frac{\theta_u}{\theta_y} \tag{6}$$

If an equal displacement approximation is assumed, the m-factor can be used to compute the maximum allowable moment demand in the linear range, i.e., multiplying m by the moment capacity M_c.

Moving now to the three-linear representation of the foundation capacity curve, this can be introduced by considering an intermediate point, corresponding to the onset of foundation uplift, denoted by (θ_{up}-M_{up}) in Figure 2. According to Crémer et al. [14] M_{up} can be computed as:

$$M_{up} = \frac{NB}{4} e^{-1.5\frac{N}{Nmax}} \quad (7)$$

and the corresponding uplift start condition is illustrated in Figure 1. Note that the ratio M_c/M_{up} ranges from 2 to 2.2 in the typical design range of N/N_{max} from 0 to 0.5. This justifies the assumption made in the ASCE 41-13 [8], where it is assumed $M_c/M_{up} = 2$. θ_{up} can easily be computed as follows:

$$\theta_{up} = \frac{M_{up}}{K_{F,0}} . \quad (8)$$

Once uplift starts, the rotational stiffness of foundation decreases as a function of the reduced base width B (see eq. 5): therefore, a reduced stiffness K_F is considered between points (θ_{up}-M_{up}) and ($\theta_{y,2}$-M_c), where $\theta_{y,2}$ is defined as the secondary yield rotation. ASCE 41-13 provides numerical values of this parameter, depending on footing shape and compression ratio, which are based on experimental evidence (see [8] and [15]).
It is important to underline that, in the region between M_{up} and M_c, the foundation response is dominated by uplift, which is a geometric non-linearity, characterized by reversibility. Therefore, footing tends to re-center at the end of excitation, with only minor permanent deformations. In this case, as shown for example by the experimental results in [1], the moment-rotation curve is characterized by typical S-shape cycles, with prevailing non-linear elasticity and small energy dissipation. On the contrary, if the moment capacity is attained during seismic excitation, significant permanent rotations and settlements may develop, with reduction of foundation stiffness and increase of energy dissipation due to plastic response [16].

Introducing in such tri-linear model the limit base moment ($M_{b,LIM}$) transmitted by the superstructure, the behavior of the integrated structure-foundation system can be preliminarily assessed as follows (Figure 3): 1) if $M_{b,LIM} < M_{up}$, the non-linear response is limited to the superstructure; 2) if $M_{up} < M_{b,LIM} < M_c$, footing uplift takes place, with minor permanent deformations at the foundation level, but, additionally, with a reduction of ductility demand on the superstructure that may be potentially significant; 3) if $M_{b,LIM} > M_c$, the non-linear response is governed by the foundation, which will provide a substantial reduction of the ductility demand on the superstructure, at the price of possible permanent damage to the foundation system itself.

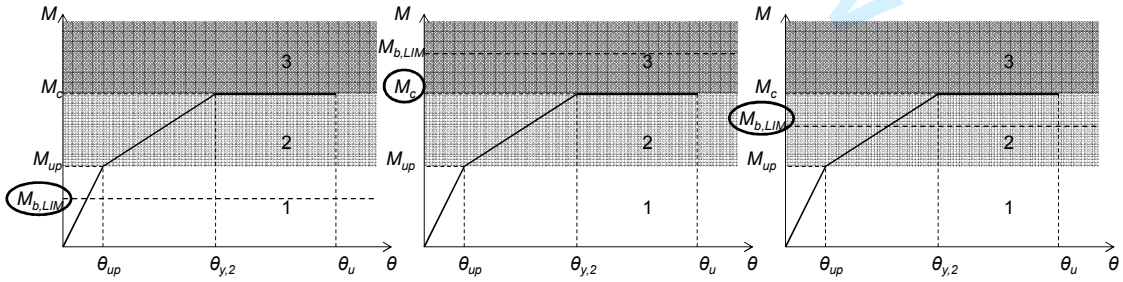

Figure 3 – Sketch to predict the response of the combined non-linear foundation-superstructure system: non-linear structure and elastic foundation (left); elastic structure and non-linear foundation (centre); balanced non-linear structure and foundation (right).

Condition 2) is typically allowed in practice, but no consideration is usually made on the amount of reduction of ductility demand on the superstructure, while condition 3) is typically avoided. However, considering the seismic assessment examples of bridge piers, falling into conditions 2) or 3), it will be shown in the following that the non-linear interaction of the foundation and super-structure plays a major role, and an integrated assessment where such interaction is accounted for may provide more rational results, in some cases avoiding uneconomic seismic retrofit strategies.

3. SEISMIC ASSESSMENT OF FOUR BRIDGE PIERS

3.1 Geometric and mechanic characteristics of the piers

To illustrate the role of the dynamic interaction of non-linear foundations and structures, the seismic assessment of four circular bridge piers lying on square shallow foundations is considered in this section. The existing bridge is assumed to have been designed in a zone for which no consideration for seismic loading was initially required. A horizontal design load V = 500 kN corresponding to 5% of the design vertical load (P = 10000 kN) was considered, to represent other design loads, such as wind and traffic. Three different values of height H were considered, namely 7.5 m for pier P1, 10 m for P2 and 5 m for P3 and P4, while two values were set for the pier diameter D: 1.5 m for P1 and P3, and 2 m for P2 and P4. Figure 4 shows the structural capacity curves resulting for the examined piers, as obtained by performing standard reinforced concrete moment-curvature analysis (see e.g. [17]). Details of pier structural characteristics are displayed in Table 1.

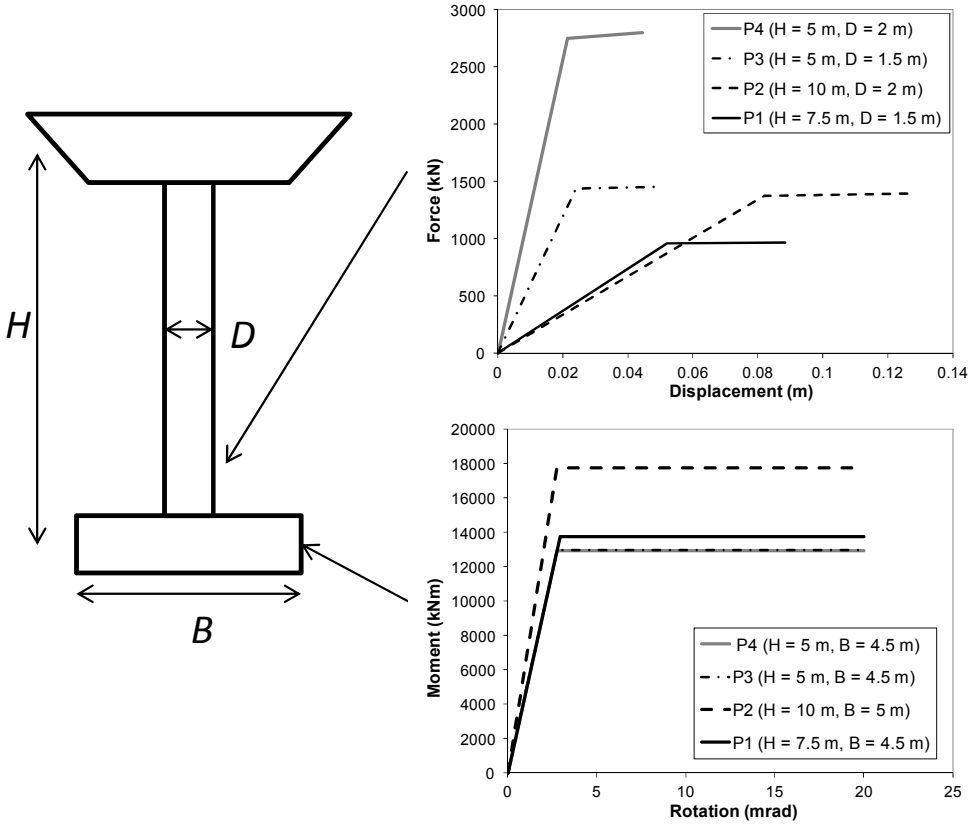

Figure 4 – Capacity curves of the four pier structures and foundations.

Table 1 – Summary of the design properties of the four piers

		P1	P2	P3	P4
Structure					
H (m)	Pier height	7.5	10	5	5
D (m)	Pier diameter	1.5	2	1.5	2
N_d (kN)	Design vertical load	10000	10000	10000	10000
$V_{b,d}$ (kN)	Design horizontal load	500	500	500	500
M_d (kNm)	Design base moment	3750	5000	2500	2500
Longitudinal rebar		20ϕ24 (ρ = 0.51%)	40ϕ24 (ρ = 0.58%)	20ϕ24 (ρ = 0.51%)	40ϕ24 (ρ = 0.58%)
Transverse rebar		ϕ12, s = 150 mm - 0.8%)	ϕ12, s = 150 mm - 0.8%)	ϕ12, s = 150 mm - 0.8%)	ϕ12, s = 150 mm - 0.8%)
Δ_y (m)	Yield displacement	0.052	0.082	0.024	0.021
$V_{b,y}$ (kN)	Yield base shear	958	1375	1436	2751
$M_{b,y}$ (kNm)	Yield moment	7185	13750	7180	13755
Δ_u (m)	Ultimate displacement	0.089	0.128	0.048	0.045
$\mu = \Delta_u / \Delta_y$	Ductility capacity	1.70	1.56	2.01	2.08
$V_{b,LIM}$ (kN)	Limit base shear	971	1398	1457	2797
$M_{b,LIM}$ (kNm)	Limit moment	7285	13984	7285	13984
K_S (kN/m)	Stiffness	18352	16797	60059	128605
T_S (s)	Structure elastic period	1.47	1.53	0.81	0.55
	Foundation				
B (m)	Foundation width	4.5	5	4.5	4.5
$K_{F,0}$ (kNm/rad)	Initial stiffness	4686000	6429000	4686000	4686000
J (tonm^2)	Centroidal moments of inertia	12710.05	12780.56	12710.05	12710.05
T_f (s)	Foundation elastic period	0.77	0.84	0.57	0.57
T_{sys} (s)	System elastic period	1.66	1.74	0.99	0.79
N_{tot} (kN)	Design vertical load	10745	10920	10745	10745
N_{max} (kN)	Static bearing capacity	28175	36316	28175	28175

FS_{vert}	Static safety factor	2.62	3.33	2.62	2.62
N/N_{max}	Compression ratio	0.38	0.30	0.38	0.38
M_c (kNm)	Moment capacity	13775	17776	12959	12959
M_{up} (kNm)	Uplift moment	6822	8694	6822	6822
θ_y (mrad)	Yield rotation	2.94	2.77	2.77	2.77
θ_u (mrad)	Ultimate rotation	20	20	20	20
θ_{up} (mrad)	Uplift rotation	1.46	1.35	1.46	1.46
$\theta_{y,2}$ (mrad)	Secondary yield rotation	14	14	14	14

In the same Table 1, the geometric dimensions and mechanical properties of the shallow foundation systems are also shown. The piers were supposed to be founded at 1.7 m depth on dense sand, characterized by a friction angle of 35° and zero cohesion, shear modulus G = 80 MPa and Poisson ratio ν = 0.3. Foundation thickness was assumed to be 1.5 m. Standard bearing capacity formulas under inclined and eccentric loads [18] were considered for design, according to the Italian standards [19]. Bi-linear capacity curves were determined also for foundations, according to the principles illustrated in the previous section. Moment capacity M_c was obtained from eq. (1), taking into account the combined effect of the horizontal base shear V. The values of allowable foundation limit rotation θ_u were determined based on ASCE 41-13 [8], where it was considered $\rho_{ac} \cong N/N_{max}$. Namely, by entering Table 8-4 of ASCE 41-13 for rectangular foundations with b/L_c = 3, and interpolating total footing rotation angle values corresponding to collapse prevention limit state, a limit foundation rotation θ_u = 20 mrad was obtained. This value is consistent also with Japanese Railway Code limit values for bridge pier rotations [13]. The resulting capacity curves for the pier foundations are shownin Figure 4. In Table 1 the values for the tri-linear approximation of the foundation capacity curves are also displayed, which will be useful in the following sections. M_{up} and θ_{up} were computed by equations (7) and (8), respectively, while secondary yield rotation $\theta_{y,2}$ was determined by interpolation of values in Table 8-4 of ASCE 41-13.

3.2 Preliminary seismic assessment under fixed-base assumption

The four piers were supposed to be subjected to seismic assessment considering the elastic spectra of acceleration and displacement shown in Figure 5, corresponding to a site in the Po Plain, Northern Italy, where seismic regulations were enforced only recently.

A preliminary simplified seismic assessment of the bridge piers was carried out by a standard uncoupled procedure, considering separately the superstructure and the foundation. For the superstructure, we used a standard equivalent elastic strength approach (see e.g., [20]), in which the elastic base shear $V_{b,el,}$ representing for the assessment the structural capacity C, is obtained from the equal displacement rule as:

$$C = V_{b,el} = \mu V_{b,LIM} \quad (9)$$

where μ is the ductility capacity of the superstructure, reported in Table 1. The elastic demand D was computed as:

$$D = V_{b,el,code} = m_S S_a(T_s) \,, \tag{10}$$

where m_S is the superstructure mass, and $S_a(T_s)$ is the spectral accelerations at the fixed-base fundamental vibration period (T_s), equal to 0.14g (T_s=1.47 s), 0.135g (T_s=1.53 s), 0.31g (T_s=0.81 s) and 0.52g (T_s=0.55 s), for P1, P2, P3 and P4, respectively. Note that we considered the fixed-base value, rather than the one with flexible base (T_{sys}), as a conservative assumption for assessment. For the same reason, we also neglected the increased damping ratio due to soil-structure interaction.

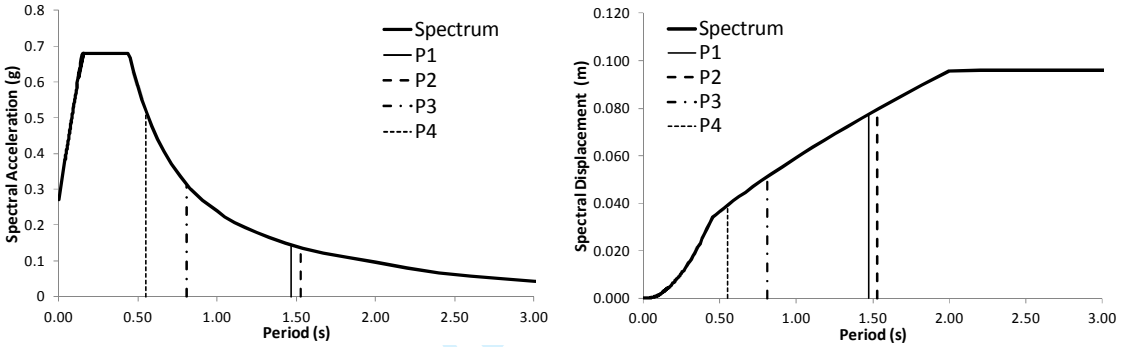

Figure 5 – Elastic acceleration (left) and displacement (right) spectra for the assessment (5% damping), and values corresponding to the fixed base periods of the four piers.

For ease of comparison with the dynamic results shown in the following, we expressed the foundation seismic assessment in terms of moment capacity ($C = M_c$) compared to moment demand calculated as the limit moment transmitted by the superstructure ($D = M_{b,LIM}$).

Results of the simplified superstructure and foundation assessment of the four piers are shown in Table 2. Piers P1, P3 and P4 result in a C/D ratio close to 1. Therefore, should a minimum safety factor FS = 1.3 be considered acceptable for the structural assessment, these piers would not pass the assessment check, at variance with pier P2. Considering now the foundation system, P4 would not pass the assessment, while P2 would be close to the 1.3 threshold.
As a result, we can say that none of the considered piers and corresponding foundations would fully pass this simplified seismic assessment, for insufficient performance either of the superstructure or of the foundation system.

Table 2 – Results of simplified seismic assessment of the four piers

	P1	**P2**	**P3**	**P4**
Structure				
S_a (g)	0.14	0.135	0.31	0.52
$V_{b,el}$ (kN)	1651	2181	2929	5818
$V_{b,el,code}$ (kN)	1400	1350	3099	5198
C/D	1.18	1.62	0.94	1.12
Foundation				
M_c (kNm)	13775	17776	12959	12959
$M_{b,LIM}$ (kNm)	7285	13984	7285	13984
C/D	1.89	1.27	1.78	0.93

4. NON-LINEAR DYNAMIC SEISMIC RESPONSE ANALYSES

In this section, we aim at verifying the performance of the interacting superstructure-foundation system, through a coupled non-linear dynamic approach. Non-linear simulations were performed by a numerical tool [21, 22], which allows one to model the combined development of non-linearities both at the structural and at the foundation level. The pier is modeled by a single degree-of-freedom (dof) oscillator (see Fig. 6), in which the non-linear response of the reinforced concrete structure is modeled by a "thin" Takeda rule [23], while the foundation is modeled by a 3 dof non-linear macro-element, as introduced in [22].

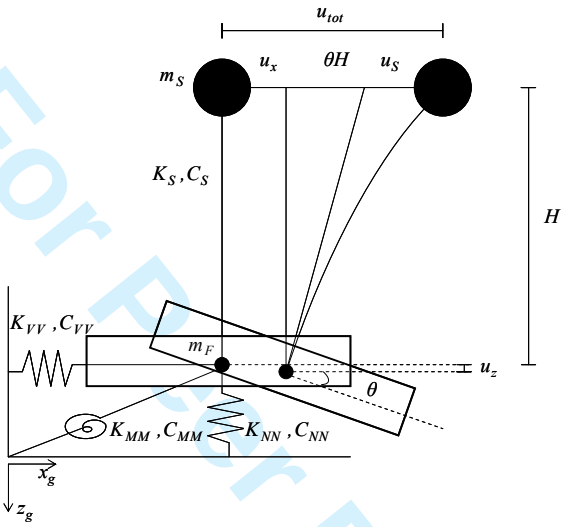

Figure 6 – Four degree-of-freedom model used for non-linear dynamic soil-structure interaction analyses.

For a comprehensive investigation of the impact of different modeling approaches of the soil-foundation system, we considered the following alternative assumptions: (1) fixed base, (2) linear elastic base (through elastic impedances), (3) non-linear macro-element model (see Fig. 6), in which both the geometric (foundation uplift) and material (soil plasticity) non-linearities are accounted for [22].

4.1 Selection of input motions for non-linear dynamic simulations

Seven accelerograms were first selected as input motion for the non-linear dynamic analyses (Figure 7, left), approaching in a broad band sense the target spectrum. Subsequently, the accelerograms were iteratively scaled in amplitude in the Fourier domain, with constant phase, until a satisfactory match with the target spectrum was obtained (Figure 7, right). With this procedure, we preserved with only slight modifications the most relevant features of the real ground motions in terms of amplitude, frequency content and duration, while keeping the compatibility with the target spectrum.

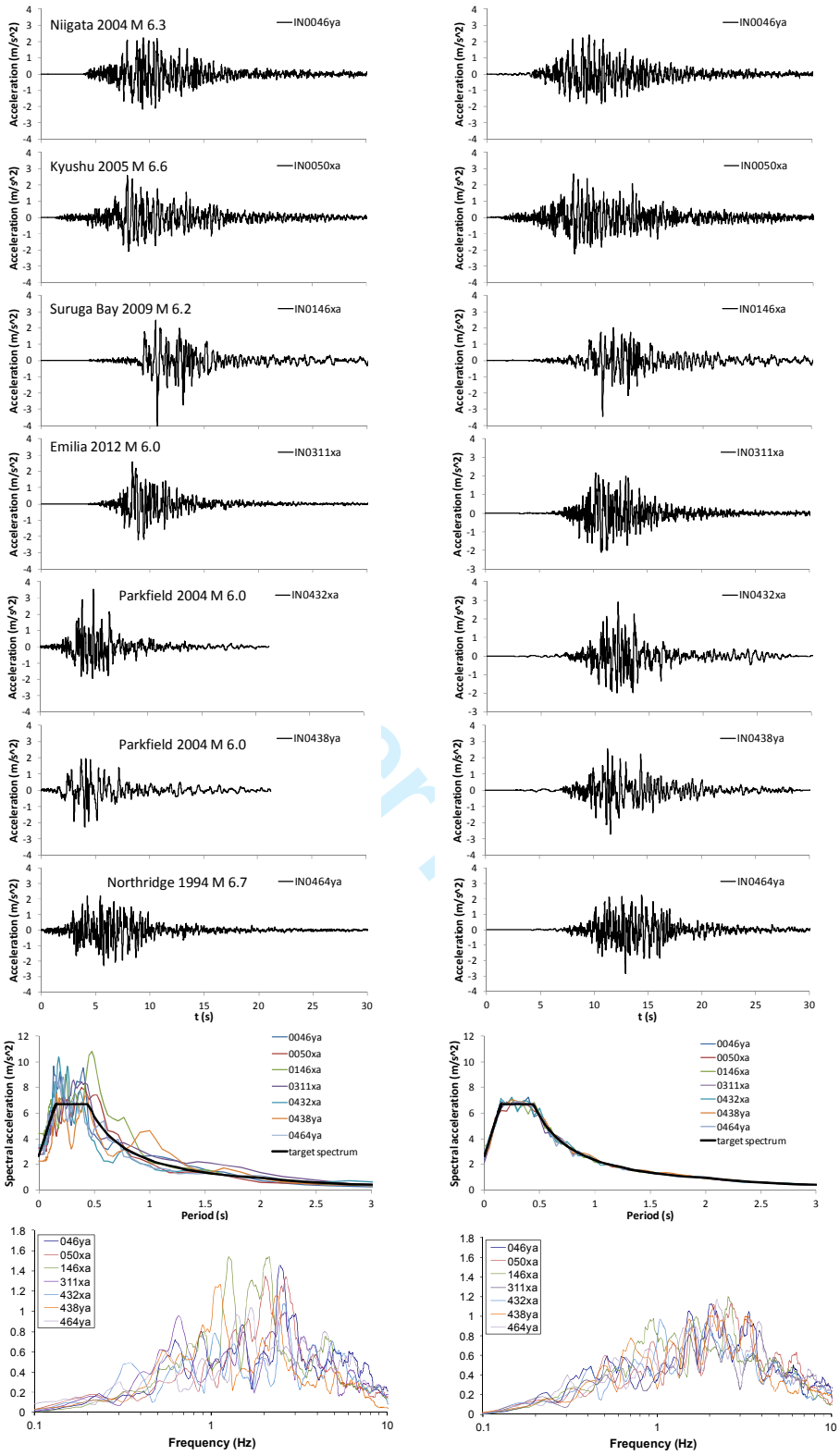

Figure 7 – Selection of seven accelerograms for dynamic analyses. Left column: original records. Right column: spectrally matched records.

4.2 Inspection of a set of results

With the objective to identify how the non-linear soil-structure interaction effects play a role on the overall system behavior of each pier, we provide in this section an overview of results of the dynamic simulations obtained with one of the previous input motions, referring to the 0438ya matched accelerogram, the time history and Fourier spectrum of which are shown in Figure 8, together with the identification of the fundamental frequencies of vibration of the fixed-base and elastic-base systems.

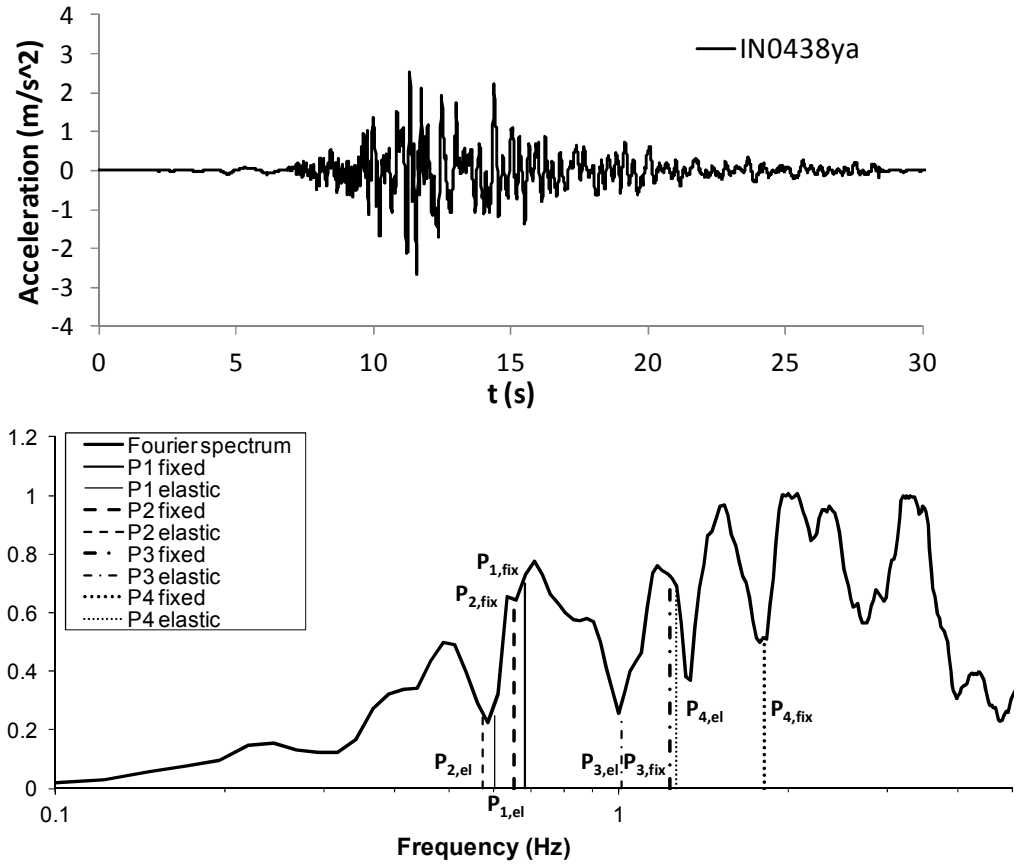

Figure 8 - Acceleration time history (top) and corresponding Fourier spectrum (bottom) considered for the investigation of numerical simulation results. On the Fourier spectrum, the fixed and elastic base natural vibration periods of the four piers are displayed.

In Figure 9 to 12 we show results for piers from P1 to P4, respectively, each figure presenting the case of fixed base (left column), linear elastic base (center) and non-linear base (right). Besides, from top to bottom, each figure presents for the superstructure: (a) base-shear vs displacement and (b) base-shear time history, while, for the foundation: (c) moment vs rotation, (d) moment time history, (e) rotation time history.

Complexity of response is clear from the inspection and comparison of the different figures, but some general remarks can be made, namely:

- dynamic soil-structure interaction is not necessarily beneficial, when considering linear elastic base, as was pointed out by Mylonakis and Gazetas [24], the amplitude of seismic response depending on details of the Fourier spectrum and its relationship with the fundamental vibration frequencies of the system;

- however, at least on average, ductility demand tends to decrease when moving from the fixed-base to the linear elastic-base case, as shown in Table 3, being mostly related to the decrease of the number of peaks of base shear with increased base flexibility;

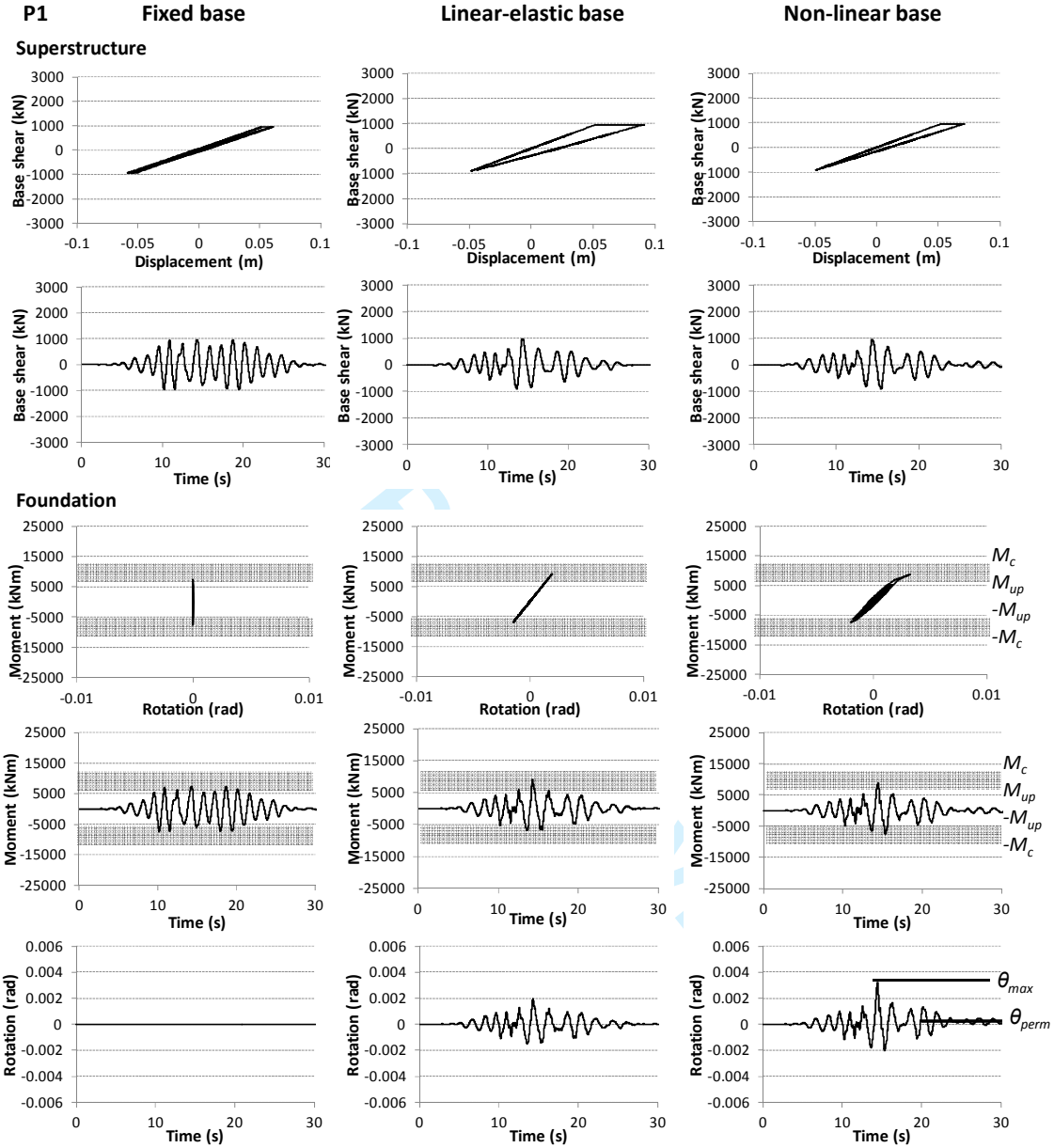

Figure 9 – Pier P1: selected responses to the input accelerogram of Figure 8 at the superstructure (top two lines) and at the foundation levels (bottom three lines), for the cases of fixed, linear-elastic and non-linear foundation.

- contrary to the fixed-base case, the moment applied to the foundation in the case of elastic base is generally larger than what would be obtained by simply multiplying the base shear by the height of the structure. More particularly, the moment time history is richer at high frequencies than the base shear time history, because of the additional contribution of the rotational inertia of the system, that would be absent for fixed base. This implies that, considering for the foundation assessment only the limit moment $M_{b,LIM}$ transmitted by the superstructure, may lead to underestimating the maximum load on the foundation;

- the structural response in the case of non-linear base presents always a substantial reduction of ductility demand on the superstructure. On the other hand, the response in terms of foundation rotation is more severe, because of increased flexibility due to uplift effects and to the presence of permanent damage expressed in terms of foundation residual rotation and settlement;
- however, for all the four piers, foundation moment capacity M_c is never attained in the non-linear base simulations: the dominant non-linear mechanism in the foundation response is uplift, as it is clear when observing the S-shape moment-rotation diagrams. Peak rotations θ_{max} are therefore larger than those calculated in the linear elastic base case, but the re-centering ability of the foundation is preserved, resulting in almost negligible values of permanent rotations θ_{perm}.

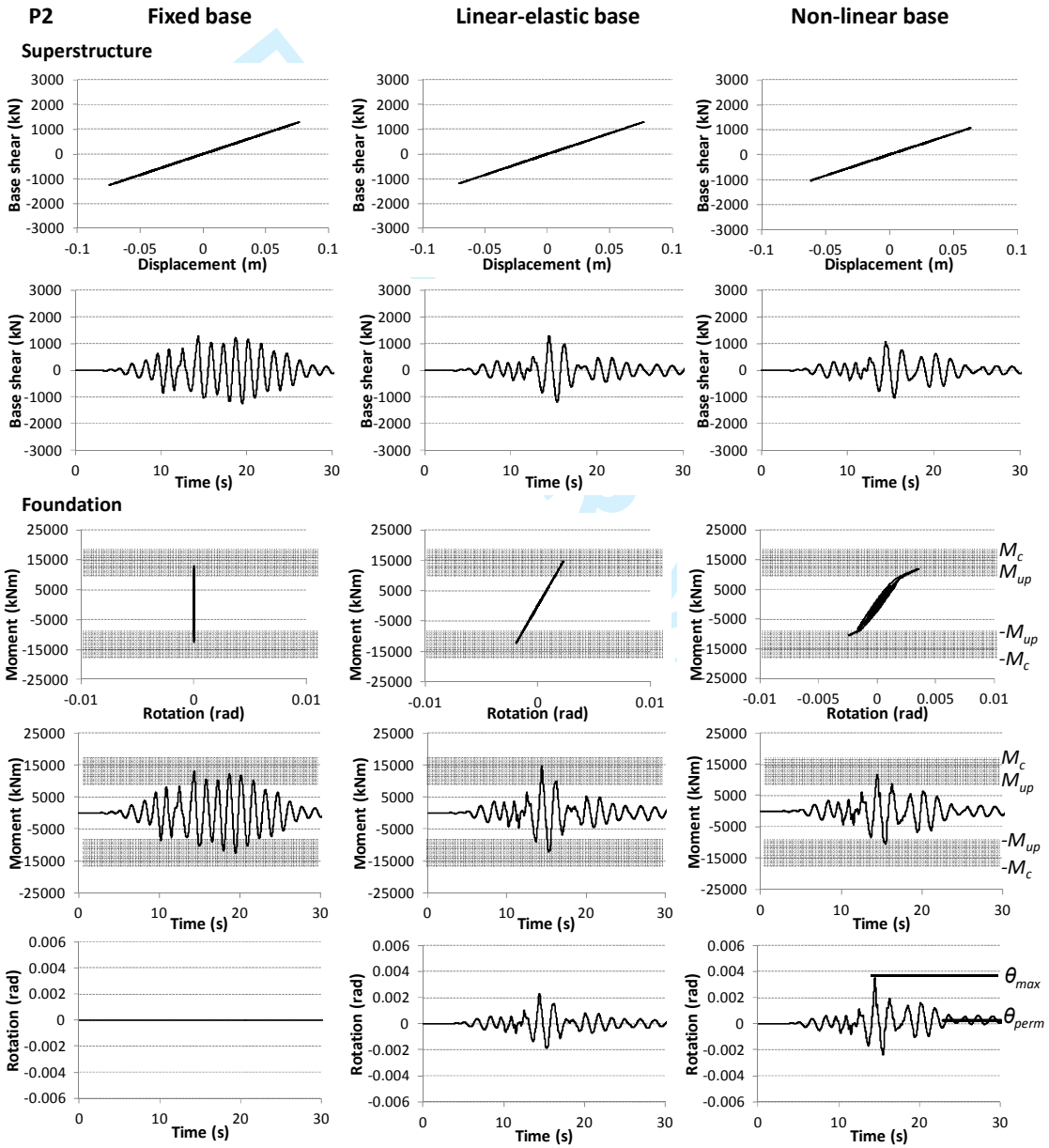

Figure 10 – Same as Fig. 9, for Pier P2

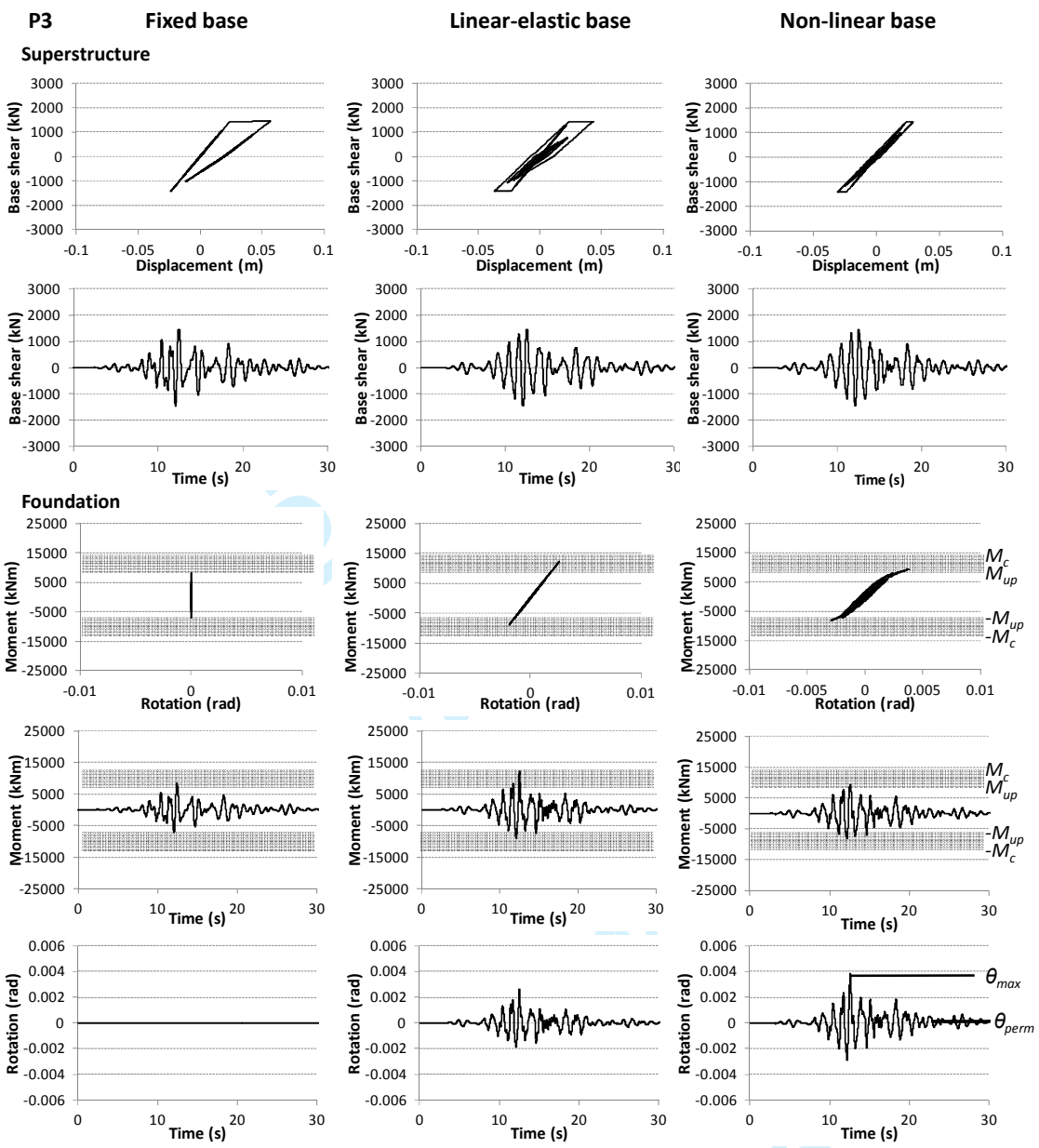

Figure 11 – Same as Fig. 9, for Pier P3

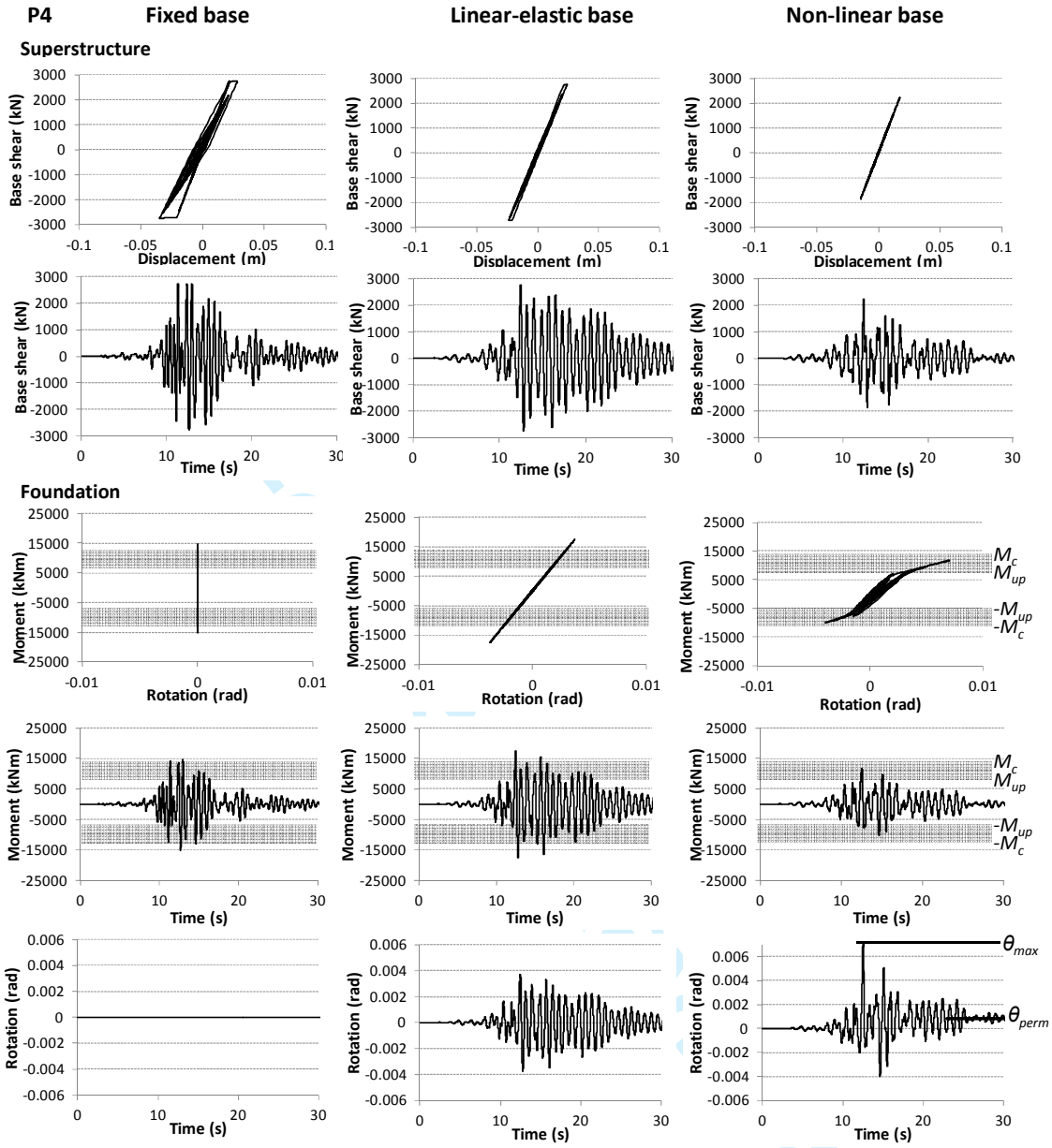

Figure 12 – Same as Fig. 9, for Pier P4

4.3 Summary of results

Selected results of the dynamic analyses performed with all the seven spectrum compatible accelerograms on the four piers are summarized in Table 3 for the three foundation models. For the superstructure, the mean values and standard deviations of simulated ductility demand μ_d and base shear V_b are shown, while, for the foundation, we display the peak rotation θ_{max} and permanent displacement (rotation θ_{perm} and settlement $u_{z,perm}$) as well as the maximum moment M_{max}.

Table 3 – Mean values and standard deviations of results obtained from dynamic simulations, together with the assessment evaluation based on simulations. In parentheses, the *C/D* evaluation from Table 2 is also reported.

Pier	Fixed base	Elastic base	Non-linear base
P1		**Structure**	
μ_d	1.45±0.15	1.42±0.16	1.20±0.10
V_b (kN)	955.2±5.9	954.3±4.7	952.8±0.9
C/D	1.17 (1.18)	1.20	1.41
		Foundation	
θ_{max} (mrad)	-	2.0±0.05	2.9±0.2
θ_{perm} (mrad)	-	-	0.23±0.15
$u_{z,perm}$ (mm)	-	-	2.1±0.5
M_{max} (kNm)	7886±242	9241±260	8509±295
C/D	1.75 (1.89)	1.49	6.90
P2		**Structure**	
μ_d	0.98±0.03	0.89±0.05	0.76±0.01
V_b (kN)	1351±32	1227±67	1042±192
C/D	1.58 (1.62)	1.75	2.06
		Foundation	
θ_{max} (mrad)	-	2.0±0.2	2.9±0.4
θ_{perm} (mrad)	-	-	0.22±0.13
$u_{z,perm}$ (mm)	-	-	1.9±0.4
M_{max} (kNm)	13680±404	13151±1002	11010±459
C/D	1.30 (1.27)	1.35	6.90
P3		**Structure**	
μ_d	2.00±0.29	1.77±0.20	1.39±0.16
V_b (kN)	1433±10	1437±9.3	1433±6.0
C/D	1.00 (0.94)	1.13	1.44
		Foundation	
θ_{max} (mrad)	-	2.4±0.2	3.5±0.4
θ_{perm} (mrad)	-	-	0.20±0.16
$u_{z,perm}$ (mm)	-	-	4.0±1.8
M_{max} (kNm)	8090±136	11072±977	9084±484
C/D	1.60 (1.78)	1.17	5.71
P4		**Structure**	
μ_d	1.61±0.08	1.31±0.24	0.76±0.09
V_b (kN)	2752±26	2745±13	2093±260
C/D	1.29 (1.12)	1.58	2.73
		Foundation	
θ_{max} (mrad)	-	4.2±0.3	6.3±0.9
θ_{perm} (mrad)	-	-	0.57±0.34
$u_{z,perm}$ (mm)	-	-	6.8±2.4
M_{max} (kNm)	15057±382	19669±1252	11297±511
C/D	0.86 (0.93)	0.66	3.2

Furthermore, the results of the superstructure and foundation assessment based on the numerical simulations are also shown in Table 3. For the superstructure, capacity over demand (*C/D*) was computed as the ratio between structural ductility capacity μ (see Table 1) and simulated

ductility demand μ_d. For the fixed and linear-elastic foundations, *C/D* was computed as the ratio of M_c and the maximum moment ($M_{\max}$) acting on the foundation from dynamic analyses. Finally, in the case of non-linear foundation *C*/*D* was computed as the ratio between limit allowable rotation θ_u and peak rotation θ_{max}.

The structural *C*/*D* results in Table 3 are in good agreement with those computed in the preliminary assessment for the fixed-base case, displayed in Table 2. Consideration of linear elastic-base slightly increases *C/D* on the superstructure, as expected because input accelerograms are matched to the target spectrum, so that demand is reduced. On the other hand, in the non-linear foundation case, a major benefit is achieved, as it can be noticed especially in the case of pier P4, where the average structural ductility demand μ_d decreases from 1.61 in the fixed base case, to 1.31 in the elastic base, down to 0.76 when considering non-linear base. This means that, in the P4 case, the superstructure response is linear and the whole input energy dissipation occurs at the foundation level. Note also that, in the non-linear foundation case, all piers show a structural *C*/*D* ratio larger than 1.3, whereas, in the simplified assessment summarized in Table 2, three of them were below that threshold.

Moving to the foundation, it can be seen from Table 3 that, while for the fixed base case the resulting *C*/*D* values approach those obtained in the preliminary uncoupled assessment, when the elastic base is considered the *C*/*Ds* are significantly smaller than in the fixed base case, except for pier P2. As noted previously, this is a consequence of the maximum moment M_{max} on the foundation being also contributed by the rotational inertia term, not present in the case of fixed-base.

Considering now the case of non-linear foundation, the *C*/*D* ratios rise significantly because foundation capacity is computed in terms of ductility, and the energy dissipation potential of the soil-foundation system is exploited. The foundation movement is moderate in terms of peak rotations, which are between 3 and 6 mrad, and almost negligible when observing residual displacements. As a matter of fact, permanent rotations are always below 1 mrad, and settlements of the order of few mm (normalized settlement $u_{z,perm}/B$ are about 0.1%). This is a consequence of the foundation response being dominated by uplift, with an almost complete re-centering at the end of the excitation. Particularly, the foundation of pier P4, which did not pass the simplified assessment, attains in the non-linear foundation case a *C*/*D* ratio by far larger than 1. This occurs at the price of limited permanent rotation (0.57 mrad) and settlement (6.8 mm) but preserving the superstructure from any damage, since its response is linear elastic. This could have been simply predicted by the sketch of Figure 3, verifying that for this pier $M_{b,LIM}$ (=13984 kNm, see Table 1) is larger than M_c (=12959 kNm). For the other piers, $M_{b,LIM}$ falls in the region between M_{up} and M_c, so that ductility demand is shared between foundation and superstructure (except for pier P2, which remains linear elastic).

A graphical summary of results is displayed in Figure 13, where the response of the four piers in terms of *C*/*D* in the superstructure (left), peak and permanent foundation rotation (center), permanent settlement (right) are compared for the different assumptions on the base response.

From the above results, we can conclude that a rational seismic assessment of existing structures, where dynamic soil-structure interaction is expected to play a role, cannot avoid considering the potential role of the non-linear foundation response and its interaction with the superstructure. In this perspective, a simplified assessment procedure such as shown in Table 2 is not expected to provide satisfactory results, since it neglects any ductility capacity of the foundation and its role in reduction of ductility demand on the superstructure.

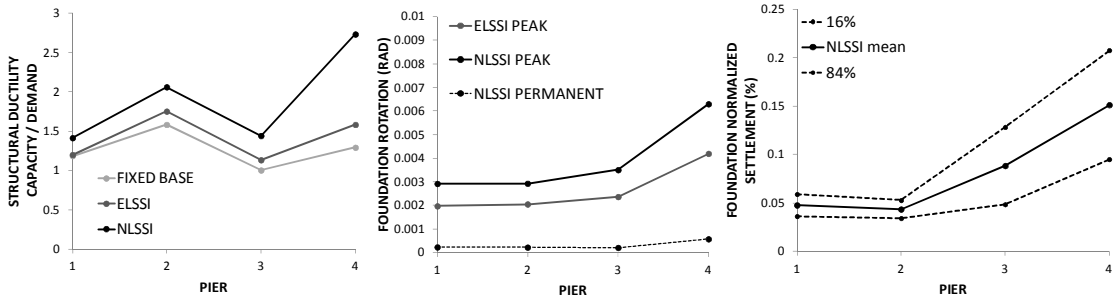

Figure 13 – Summary of dynamic analysis results of the four piers: structural capacity over demand (left), peak and permanent foundation rotations (center) and normalized foundation settlements (right).

A reasonable improvement is obtained when foundation ductility factors (denoted as *m*-factors in FEMA 356 and ASCE 41-13, see eq. (6)) are considered. For this purpose, the elastic moment capacity *C* can be estimated as:

$$M_{el} = mM_c \tag{11}$$

while the elastic moment demand *D* can be computed as:

$$M_{el,code} = V_{b,el,code}H \tag{12}$$

Results of such simplified assessment procedure, applied to the piers under study, are compared in Table 4 with those obtained by dynamic analyses, shown in Table 3. In this case, *C*/*D* ratios for foundations are in reasonable agreement with numerical results, especially for piers P3 and P4.

Table 4 – Results of the alternative simplified seismic assessment of the four foundations, based on foundation ductility factors *m*. In parentheses, the *C/D* ratios obtained by dynamic analyses of the non-linear foundation system, shown in Table 3 for the case of non-linear base.

	P1	**P2**	**P3**	**P4**
		Foundation		
m	6.8	7.2	7.2	7.2
M_{el} (kNm)	93670	127987	93305	93305
$M_{el,code}$ (kNm)	10500	13500	15495	25990
C/D	8.9 (6.9)	9.5 (6.9)	6 (5.7)	3.6 (3.2)

We finally remark that, although these results strongly support the use of simplified assessment procedures that account for foundation ductility factors, such as proposed in the Chapter 8 of ASCE 41-13, such procedures are still affected by the drawback of treating the foundation and the superstructure as uncoupled systems, so that they neglect the interaction of the two subsystems. In this sense, while the approach based on ductility factors improves substantially the agreement with the results of non-linear simulations at the foundation level, it does not change the superstructure assessment results shown in Table 2. The introduction of a fully coupled seismic assessment procedure is beyond the scope of this paper, but its development is presently under way, following a similar iterative procedure as proposed by [4], within the

framework of an integrated displacement-based design procedure of the foundation-superstructure system.

5. CONCLUSIVE REMARKS

The impact of the ductility capacity of the soil-foundation system in the seismic assessment of structures was highlighted in this paper. For this purpose, reference was made to a set of four bridge piers lying on shallow foundations, which were not designed to withstand earthquake loading. Because of low safety factors, either at the foundation or at the superstructure level, none of the four piers would have complied with a simplified seismic assessment based on capacity design principles, which disregards the ductility capacity of the foundation and its impact on the response of the superstructure.

After this preliminary check, a set of non-linear dynamic simulations was performed, considering a simplified model of the piers, consisting of a non-linear single degree-of-freedom structure over a three-degrees-of-freedom foundation, represented by a non-linear macro-element, which accounts for both uplift and plastic response of the soil-foundation system. The numerical simulations were carried out by considering a set of real accelerograms scaled to match the target response spectrum used for the assessment, and different assumptions on the foundation response were made, namely a) fixed base; b) linear-elastic base; c) non-linear base.

Some interesting features were highlighted by the numerical simulations, which clearly pointed out the complexity of the interaction between the foundation and the superstructure, both modelled as non-linear systems. Besides, the role of the non-linear foundation response to substantially reduce the ductility demand on the superstructure was clarified by the numerical simulations, confirming the evidence of a large set of recent experimental results. This role is effective especially when the foundation takes advantage of its ability for partial uplift, which, thanks to re-centering, allows the foundation to develop only a limited amount of permanent deformation, both in terms of rotation and settlement. For example, in the case of pier P4 which would not have passed the simplified seismic assessment not accounting for foundation ductility capacity, ductility demand on the superstructure was reduced by more than a factor of 2, turning to a fully linear response, while the foundation was characterized by limited peak rotations (about 0.6%) and negligible permanent rotation (0.05%) and vertical settlement (6 mm, i.e., about 0.15% of the foundation width).

Although non-linear dynamic analyses pointed out that the comparison of structure and foundation capacities is not sufficient alone to predict the global performance of the interacting system, it was found that a simplified assessment procedure of the foundation which accounts for ductility factors, such as introduced in Chapter 8 of ASCE 41-13, may reasonably approach the results of dynamic analyses, at least for the foundation sub-system. However such procedures, that do not account for the coupling of the foundation and superstructure subsystems, are not suitable to predict the reduction of ductility demand at the superstructure level due to non-linear foundation response.

A more advanced assessment procedure is presently under development which, rather than relying on the classical approach of uncoupling the foundation assessment from that of the superstructure, aims at accounting for the interaction of the two sub-systems by iterative steps, following a similar procedure as introduced in [4] for the integrated displacement-based design of the foundation-superstructure system.

REFERENCES

1. Pecker A, Paolucci R, Chatzigogos C, Correia AA, Figini R. The role of non-linear dynamic soil-foundation interaction on the seismic response of structures. *Bulletin of Earthquake Engineering* 2014; **12**: 1157-1176. DOI: 10.1007/s10518-013-9457-0.
2. Anastasopoulos IM, Loli Georgarakos T, Drosos V. Shaking table testing of rocking-isolated bridge pier on sand. *Journal of Earthquake Engineering* 2013; **17**:1–32.
3. Deng L, Kutter BL, Kunnath S. Centrifuge modeling of bridge systems designed for rocking foundations. *ASCE Journal of Geotechnical and Geoenvironmental Engineering* 2012; **138**: 335–344.
4. Paolucci R, Figini R, Petrini L. Introducing dynamic non-linear soil-foundation-structure interaction effects in displacement-based seismic design. *Earthquake Spectra* 2013; **29** (2): 475-496. DOI: 10.1193/1.4000135.
5. Deng L, Kutter BL, Kunnath SK. Seismic Design of Rocking Shallow Foundations: Displacement-Based Methodology. *ASCE Journal of Bridge Engineering*, 2014; DOI: 10.1061/(ASCE)BE.1943-5592.0000616.
6. Gazetas G. 4th Ishihara lecture: Soil–foundation–structure systems beyond conventional seismic failure thresholds. *Soil Dynamics & Earthquake Engineering* 2015; **68**: 23-39.
7. Liu W, Hutchinson TC, Kutter BL, Hakhamaneshi M, Aschheim MA, Kunnath SK. Demonstration of Compatible Yielding between Soil-Foundation and Superstructure Components. *ASCE Journal of Structural Engineering* 2013; **139** (8): 1408-1420.
8. Kutter BL, Moore M, Hakhamaneshi M, Champion C. Rationale for shallow foundation rocking provisions in ASCE 41-13. *Earthquake Spectra* in press; DOI: http://dx.doi.org/10.1193/121914EQS215M.
9. Nova R, Montrasio L. Settlement of shallow foundations on sand. *Geotechnique* 1991; **41**(2): 243–256.
10. Vesic AS. Bearing Capacity of Shallow Foundations. *Foundation Engineering Handbook*, Winterkorn HF, Fang HY (eds), Van Nostrand Reinhold: New York, 1975; 121–147.
11. Adebar P. Nonlinear Rotation of Capacity-Protected Foundations: The 2015 Canadian Building Code. *Earthquake Spectra* 2015; **31** (4): 1885-1907.
12. Gazetas G. Foundation Vibrations. *Foundation Engineering Handbook*, Chapter 15 (2nd edn), Fang H-Y (ed.). V.N. Reinhold: New York, 1991; 553–593.
13. Japan Road Association. Design Specifications for Highway Bridges 2002.
14. Crémer C, Pecker A, Davenne L. Cyclic macro-element for soil-structure interaction: material and geometrical nonlinearities. *International Journal for Numerical and Analytical Methods in Geomechanics* 2001; **25**:1257–1284. DOI: 10.1002/nag.175.
15. Hakhamaneshi M, Kutter BL, Moore M, Champion C. Validation of ASCE 41-13 modeling parameters and acceptance criteria for rocking shallow foundations. *Earthquake Spectra* in press; DOI: http://dx.doi.org/10.1193/121914EQS216M.
16. Paolucci R, Shirato M, Yilmaz MT. Seismic behaviour of shallow foundations: shaking table experiments vs. numerical modelling, *Earthquake Engineering & Structural Dynamics* 2008, **37**: 577-595.
17. Priestley MJN, Calvi GM, Kowalski MJ. *Displacement Based Seismic Design of Structures* 2007, IUSS Press, Pavia, Italy.
18. Brinch Hansen J. A revised and extended formula for bearing capacity. *The Danish Geotechnical Institute bulletin* 1970; **28**, Copenhagen.
19. Ministero delle Infrastrutture. D. Min. Infrastrutture 14 Gennaio 2008. Nuove norme tecniche per le costruzioni. *Gazzetta Ufficiale della Repubblica Italiana* 2008; **29**

20. ASCE. FEMA 356 - Prestandard and commentary for the seismic rehabilitation of building. *Federal Emergency Management Agency* 2000.
21. Figini R. Non-linear dynamic soil-structure interaction: application to seismic analysis and design of structures on shallow foundations. *PhD Thesis*, Politecnico di Milano, Italy, 2010.
22. Figini R, Paolucci R, Chatzigogos CT. A macro-element model for non-linear soil-shallow foundation-structure interaction under seismic loads: theoretical development and experimental validation on large scale tests. Earthquake Engineering and Structural Dynamics 2012; **41**(3): 475–493. DOI: 10.1002/eqe.1140.
23. Takeda T, Sozen MA, Nielsen NN. Reinforced Concrete Response to Simulated Earthquakes. *ASCE Journal of Structural Engineering* 1970; **96** (12).
24. Mylonakis G, Gazetas G. Seismic soil-structure interaction: beneficial or detrimental?. Journal of Earthquake Engineering 2000; **4**(3): 277-301.